Subcritical Turing bifurcation and the morphogenesis of localised patterns

Víctor Breña–Medina[1,2] & Alan Champneys[2]

[1]*Departamento de Nanotecnología, Centro de Física Aplicada y Tecnología Avanzada,*
Universidad Nacional Autónoma de México, Juriquilla No. 3001, Querétaro 76230, México
[2]*Department of Engineering Mathematics, University of Bristol,*
Queen's Building, University Walk, Bristol BS8 1TR, United Kingdom

(Dated: September 10, 2014)

Subcritical Turing bifurcations of reaction-diffusion systems in large domains lead to spontaneous onset of well-developed localised patterns via the homoclinic snaking mechanism. This phenomenon is shown to occur naturally when balancing source and loss effects are included in a typical reaction-diffusion system, leading to a super/subcritical transition. Implications are discussed for a range of physical problems, arguing that subcriticality leads to naturally robust phase transitions to localised patterns.

I. INTRODUCTION

Reaction-diffusion systems are known to give rise to a wide variety of stationary and oscillatory patterns, see e.g. [1–3]. The primary mechanisms for explaining transition from quiescent to patterned states is the instability first described by Alan Turing [4]. Such patterns are used to explain diverse physical phenomena, such as gas discharge dynamics [5], active fluid behaviour [6] and tumour growth [7]. Now diffusion-driven instability, or *Turing bifurcation*, is a key part of any graduate course on nonlinear far-from equilibrium physics or biology. For systems in large domains however, many different wave numbers can become unstable in Turing bifurcations for nearby parameter values and mode interactions can lead to a remarkable richness in patterns and their dynamics, see e.g. [8].

A different explanation of *localised* pattern formation has emerged in recent years; the so-called homoclinic snaking mechanism [9, 10]. The 1D generalised Swift–Hohenberg equation with competing nonlinear terms is a canonical model for such analysis [11, 12]. In 2D a richness of localised stripy, spotty, hexagonal, square-wave and target-like patterns have been observed [13–15]. The mechanism has been shown to underlie many physical observations such as the onset of turbulent spots in plain Couette flow [16], stationary patterns in binary convection [17] and localised modes in optical cavities [18].

One of the distinctions between the homoclinic snaking and Turing bifurcation pattern formation theories is that the Swift–Hohenberg equation has variational structure, which can be linked to the free energy of the system. General systems of reaction diffusion equations for which the Turing mechanism applies do not typically have such variational structure. However, the snaking mechanism still applies to Swift–Hohenberg equations with broken variational structure [19], provided spatial reversibility is retained, albeit stationary asymmetric patterns are lost.

The purpose of this paper then is to show how the connection between homoclinic snaking and Turing instability analysis gives a robust explanation for the formation of localised patterns in reaction-diffusion systems. We show that this robustness arises from inclusion of source and loss terms in reaction-diffusion models, which realistic effects are often ignored in canonical models. For example, a model equivalent to the system we study below but without source and loss terms gives rise to wave pinning but no localised patterns [20]. Inclusion of such terms naturally breaks material conservation, paves the way for effective competing nonlinear terms and in turn this allows Turing bifurcations to become *sub-critical*. We show that this subcriticality is equivalent to the key condition for homoclinic snaking to occur in long domains (see also [13]). Hence, upon considering long domains, we can set the backbone conditions under which reaction-diffusion systems naturally give rise to spots and pulses, rather to than just spatially extended patterns (see also [3] for further experimental and theoretical evidence).

It is worth mentioning earlier related work of Yochelis *et al.* [21] who performed numerical bifurcation analysis on the Gierer–Meinhardt system, which includes a rational nonlinearity. They also found the existence of a bistability region and a subcritical Turing bifurcation that leads to homoclinic snaking; see also [22] for further details. The novelty of the present paper is to show that such scenarios are in some sense generic and can occur for a pure-power nonlinear system, given the presence of source and loss terms.

II. LOCAL ANALYSIS

For the ease of explanation, we shall perform our detailed calculations in 1D in space. Extension to higher spatial dimension is in principle possible as we shall indicate in what follows, although there are additional considerations due to the range of different spatial symmetries of underlying patterns, stripes, rolls, hexagonal lattices, among others, see [14, 15, 23]. We shall also apply the theory to reaction-diffusion systems with just two interacting species and a single nonlinear interaction term. Application to more complex systems is in principle straightforward, because the theory is built upon the principle of normal-form reduction.

Consider a reaction-diffusion system

$$U_t = D_1 U_{xx} + F(U, V; \mu)\,, \qquad (1a)$$
$$V_t = D_2 V_{xx} + G(U, V; \mu)\,, \qquad (1b)$$

for $x \in (-L/2, L/2)$, subject to homogeneous Neumann boundary conditions. Here, parameters D_1 and D_2 are diffusion coefficients and F and G are sufficiently smooth functions. Without loss of generality timescales have been scaled to unity, but the length scale L is retained.

The linear analysis provides of the usual conditions under which Turing bifurcations occur, see [2]. Thus, suppose there exists an isolated homogeneous equilibrium $(U, V)^T = (U_0, V_0)^T$. Upon substituting the incremental variables $U = U_0 + u$ and $V = V_0 + v$ into system (1), we obtain

$$\begin{pmatrix} u_t \\ v_t \end{pmatrix} = \begin{pmatrix} D_1 u_{xx} \\ D_2 v_{xx} \end{pmatrix} + \mathbf{A}(\mu) \begin{pmatrix} u \\ v \end{pmatrix} + \begin{pmatrix} f(u, v; \mu) \\ g(u, v; \mu) \end{pmatrix} \qquad (2)$$

where $\mathbf{A} = \{a_{ij}\}$ with $a_{11}(\mu) = F_U$, $a_{12}(\mu) = F_V$, $a_{21}(\mu) = G_U$, $a_{22}(\mu) = G_V$ evaluated at the steady state and f and g gather all remaining higher-order terms. Under the usual assumptions of Turing bifurcation analysis, we first need to assume that the homogeneous steady state is stable in the absence of diffusion; that is trace $\mathbf{A} < 0$ and det $\mathbf{A} > 0$.

To find diffusion-driven instability with spatial wavenumber κ we look for modes of the form

$$\cos\left(\kappa(x - L/2)\right) \begin{pmatrix} C_1 \\ C_2 \end{pmatrix}, \quad C_1^2 + C_2^2 > 0\,, \qquad (3)$$

where $\kappa = \kappa_m = m\pi/L$ for some positive integer mode number m. This leads to the search for zero eigenvalues λ of the matrix

$$\mathbf{A}_\kappa(\mu) = \begin{pmatrix} a_{11} - D_1\kappa^2 & a_{12} \\ a_{21} & a_{22} - D_2\kappa^2 \end{pmatrix}, \qquad (4)$$

with wavenumber $\kappa = \sqrt{(D_2 a_{11} + D_1 a_{22})/(D_1 D_1)}$. The condition for instability is that κ is real, which is guaranteed for a stable equilibrium (with sign $(a_{11}a_{22}) < 0$) if $D_1 D_2 \ll \max\{D_1^2, D_2^2\}$. Without loss of generality, suppose $a_{22} < 0$ and that $D_1 \ll D_2$ which, in comparison to the V component, implies that the U component diffuses slowly.

We now perform a proper comparison between the two theories in question, in the case of a long domain $L \gg 1$. We suppose that at parameter value $\mu = \mu_c$ there is a double zero eigenvalue of A_κ, corresponding to a large mode number m_c, not necessarily an integer. The condition for such a double root is

$$(D_2 a_{11} + D_1 a_{22})^2 = 4 D_1 D_2 \det \mathbf{A}. \qquad (5)$$

On the one hand, for a $L \gg 1$ there will be a large number of Turing bifurcations for nearby κ-values corresponding to $\kappa = m\pi/L$ for integers m close to m_c. Generically, μ will depend quadratically on κ close to μ_c, which would
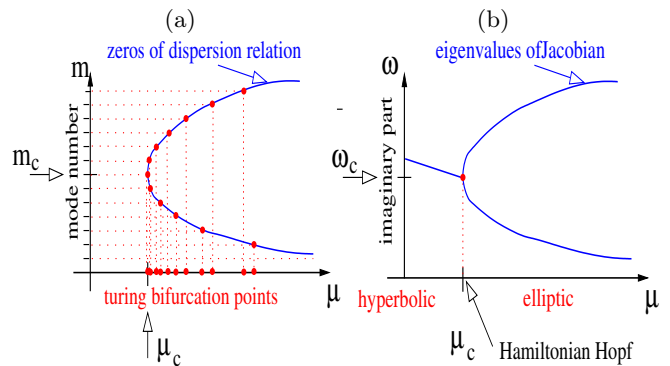

FIG. 1. (Color online) The equivalence between (a) the mode numbers accumulation point of Turing bifurcations and (b) a Hamiltonian–Hopf bifurcation point for long domains.

imply a double accumulation of Turing bifurcations; one family corresponding to higher wavenumbers $\kappa > \kappa_c$, the other to lower wavenumbers $\kappa < \kappa_c$; see in Fig. 1(a) the mode numbers m which correspond to zeros of the dispersion relation as μ tends towards μ_c.

Alternatively, in the limit $L \to \infty$, so-called spatial dynamics can be applied (see e.g. [9]) where steady states $(U(x, t), V(x, t))^T = (u(x), v(x))^T$ of (1) are sought by considering the ODE system on the real line

$$D_1 u_{xx} + F(u, v; \mu) = 0\,, \quad D_2 v_{xx} + G(u, v; \mu) = 0\,,$$

as a four-dimensional dynamical system in 'time' x. As such, the symmetry $(u_x, v_x)^T \to (-u_x, -v_x)^T$ and $x \to -x$ corresponds to a spatial reversibility. In this context, a homogeneous steady state $(U_0, V_0)^T$ of the PDE corresponds to an equilibrium $(u, u_x, v, v_x)^T = (U_0, 0, V_0, 0)^T$ within the fixed point set of the reversibility. The linearisation of the system about such an equilibrium would take the form

$$\begin{pmatrix} u_{xx} \\ v_{xx} \end{pmatrix} + \begin{pmatrix} a_{11}/D_1 & a_{12}/D_1 \\ a_{21}/D_2 & a_{22}/D_2 \end{pmatrix} \begin{pmatrix} u \\ v \end{pmatrix} = \begin{pmatrix} 0 \\ 0 \end{pmatrix}. \qquad (6)$$

Such an equilibrium will undergo a transition from being hyperbolic to elliptic at a Hamiltonian–Hopf bifurcation (also known as a reversible 1:1 resonance) [24] which occurs, under suitable non-degeneracy conditions, when there is a double pair of complex conjugate eigenvalues $\pm i\omega$ of the Jacobian in (6). Upon substituting $(u, v)^T = (A, B)^T \exp(i\omega x)$ into (6), we find that we need a double root to

$$D_1 D_2 \omega^4 - (D_2 a_{11} + D_1 a_{22})\omega^2 + \det \mathbf{A} = 0\,,$$

which leads to precisely the same condition for a fold Turing points with respect to κ, namely equality as in (5); see Fig. 1(b). It is straightforward to show that the condition for a criticality of the Turing bifurcation at the double root is precisely the same as the condition for the criticality of the corresponding Hamiltonian–Hopf;

see e.g. [25]. Both problems may be expressed as via an amplitude equation whose real part reads [24]

$$Z''(\xi) = q_1(\mu - \mu_c)Z + q_3 Z|Z|^2 + q_5 Z|Z|^4 \,. \quad (7)$$

A key prediction of the homoclinic snaking mechanism [10] is the birth of a spatially localised mode (a homoclinic orbit in space x) if the Hamiltonian–Hopf bifurcation is subcritical, $q_1 q_3 > 0$. For small $q_1 q_3 > 0$, then, provided $q_1 q_5 < 0$, an unfolding of the normal form shows that there is a heteroclinic connection from a background state to a non-trivial periodic orbit. Taking account of beyond-all-orders terms in the normal form [26, 27] enables an analysis to be undertaken in which we find infinitely many homoclinic orbits arranged on two closed curves; see Fig. 3(b), below.

III. ILLUSTRATION FOR A GENERALISED SCHNAKENBERG SYSTEM

In order to illustrate our findings, we here consider the generalised Schnakenberg system, which is a spatially homogeneous form of a model proposed in [28] of pattern formation via interaction between active U and inactive V small G-proteins in sub-cellular-level biological morphogenesis:

$$U_t = D_1 \nabla^2 U + k_2 U^2 V - (c+r)U + hV \,, \quad (8a)$$
$$V_t = D_2 \nabla^2 V - k_2 U^2 V + cU - hV + b \,, \quad (8b)$$

in which all parameters are taken to be positive. Here the model models a non-reversible autocatalytic process, and differs from the standard Schnakenberg and Gray–Scott systems through the presence of a production term b of the inactive component and removal rate r of the activated component. Notice that, as can easily be shown, otherwise Turing bifurcations are always supercritical in straightforward Schnakenberg and Gray–Scott systems.

There is a unique homogeneous equilibrium

$$U_0 \equiv \frac{b}{r} \,, \qquad V_0 \equiv \frac{br(c+r)}{k_2 b^2 + hr^2} \,. \quad (9)$$

Upon substituting the incremental variables $U = U_0 + u$ and $V = V_0 + v$ into system (8) in 1D, we get a system of the form (2) where the coefficients of $\mathbf{A}$ are given by

$$a_{11} = \frac{(c+r)\left(k_2 b^2 - hr^2\right)}{k_2 b^2 + hr^2} \,, \quad (10a)$$

$$a_{12} = -a_{22} = \frac{k_2 b^2 + hr^2}{r^2} \,, \quad (10b)$$

$$a_{21} = \frac{chr^2 - k_2 b^2 \left(c + 2r\right)}{k_2 b^2 + hr^2} \,. \quad (10c)$$

and the nonlinear terms

$$\begin{pmatrix} f \\ g \end{pmatrix} \equiv k_2 \left(u^2 v + V_0 u^2 + 2U_0 uv\right) \begin{pmatrix} 1 \\ -1 \end{pmatrix} \,. \quad (11)$$
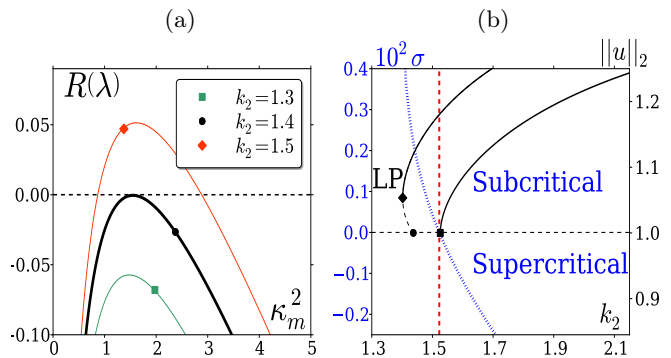

FIG. 2. (Color online) (a) Dispersion relation of $\mathbf{A}_\kappa(\mu)$ restricted to the eigenspace spanned by modes of the form (3). The bold solid curve corresponds to where a double root of $\det[\mathbf{A}_\kappa(\mu)] = 0$ occurs. (b) Bifurcation diagram and pitchfork criticality condition; stable branches are shown as solid lines, the filled circle at $k_2 = 1.4369$ corresponds to a subcritical bifurcation, and the square at $k_2 = 1.5258$ to a supercritical bifurcation. The subcritical branch undergoes to a fold bifurcation (LP). The pitchfork criticality condition is depicted as a (blue) heavily dashed line, where the criticality transition is indicated by a (red) vertical dashed line at $k_2 = 1.5226$.

Note that the nonlinearity contains both quadratic and cubic terms when written in these co-ordinates. It is straightforward to show that the steady state $(U_0, V_0)^T$ is asymptotically stable in the absence of diffusion provided $c + r < 8h$.

Fig. 2(a) shows the dispersion relation as function of squared wavenumber κ_m^2, for several values of a bifurcation parameter k_2. In this and unless otherwise stated in what follows we use parameter values $k_2 \in (0, 5)$ and $b = 1$, $c = 1$, $r = 1$, $h = 1$, $D_1 = 0.1$, $D_2 = 10$.

To calculate the criticality condition of the Turing instabilities of (8), we follow a Lyapunov–Schmidt reduction method [29]. Upon obtaining the steady-state smooth functional $\boldsymbol{\phi} = \boldsymbol{\phi}(U, V, \mu)$, which comes from setting u_t and v_t to zero, and hence defining the bifurcation function $g(z, \mu) \equiv \langle \mathbf{w}^*, \boldsymbol{\phi}(z\mathbf{w}, \mu) \rangle$ at the steady-state $\mathbf{w} = (u - U_0, v - V_0)^T$, the result is a so-called bifurcation equation $g = 0$, the leading-order expansion of which can be written

$$g(z, \mu) = q_1 \mu z + q_3 z^3 + q_5 z^5 + \mathcal{O}\left(\mu^2 z, \mu z^3\right) \,. \quad (12)$$

Note that the form of g is identical to the right-hand side of the amplitude equation (7). The bifurcation parameter here is defined as $\mu = k_2 - k_{2c}$ and the scalar variable z parametrises the amplitude of the component of the Turing pattern in the kernel of the matrix $\mathbf{A}_\kappa(\mu) = -\mathbf{D}\kappa^2 + \mathbf{A}$, where $\mathbf{D}$ is the diffusivity matrix. The calculation of the coefficients q_i is straightforward but lengthy, full details are available in [30], we omit the details for brevity.

Note that such bifurcation equation (12) can be derived in principle in a higher dimensional spatial domain Ω.
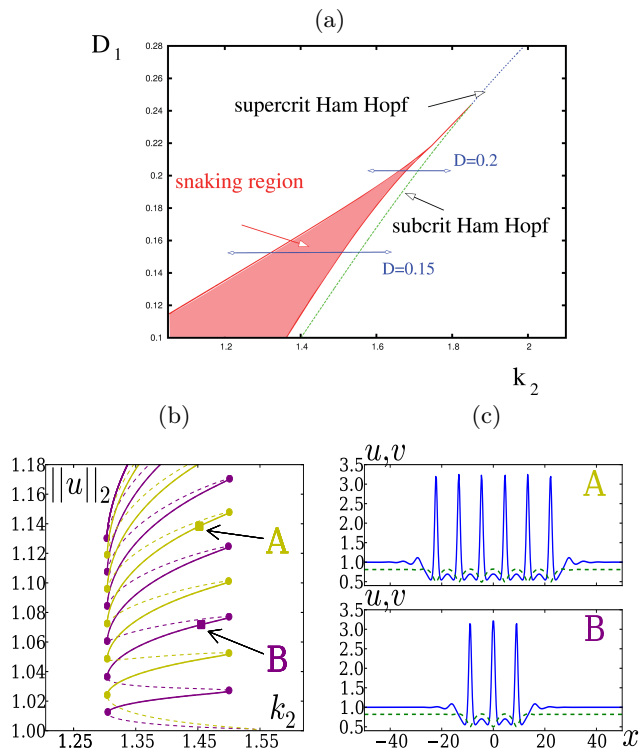
FIG. 3. (Color online) (a) The snaking region (shaded) inside which homoclinic snaking is observed in the (k_2, D_1) parameter plane. (b) Homoclinic snaking; even-solutions branch (yellow) and odd-solutions branch (purple), and fold bifurcations (filled circles); bold solid lines indicate stable branches; $D_1 = 0.15$. (c) Samples of multi-pulse homoclinic stable solutions on the even- and odd-branch for $k_2 = 1.45$, top and bottom panels respectively, which correspond to 6-spike solution (label A) and 3-spike solution (label B) in (b). The u-component (solid line) and v-component (dashed line) are plotted for a domain size $L = 100$.

There, a vector reduced bifurcation function **g** can be computed by projecting onto the eigenspace defined by modes satisfying the boundary value problem

$$\nabla^2 \mathbf{w} + |\boldsymbol{\kappa}|^2 \mathbf{w} = \mathbf{0}, \quad (\mathbf{n} \cdot \nabla) \mathbf{w}|_{\partial\Omega} = \mathbf{0}.$$

In computing the scalar function g, we find that trivially $g_\mu(0,0) = 0$ and $g_{\mu\mu}(0,0) = 0$, by virtue of the equilibrium being at the origin and having a zero eigenvalue. Also, owing to the reflection symmetry in x, the reduced bifurcation function must be odd in z, despite the presence of quadratic terms in the original equation.

In the parameter region under investigation the sub/super-criticality of the pitchfork (Hamiltonian–Hopf) bifurcation is determined by the sign of

$$\sigma = q_1 q_3,$$

see [24]. Figure 2(b) plots σ, as a function of k_2 close to k_{2c}. We have also checked that $q_1 q_5$ is negative in all the entire parameter region of interest. The figure also

shows computed bifurcating branches close to the point where σ changes sign, where we can see a re-stabilising fold (limit point) in the case of the sub-critical bifurcation.

Now consider variation of a second parameter. For convenience we choose D_1. Figure 3(a) depicts a two-parameter bifurcation diagram showing the Hamiltonian–Hopf bifurcation curve, the codimension-two point at which $\sigma = 0$ and the numerically computed "snaking region" in which localised states exist in the (k_2, D_1) plane. In accordance with the usual analysis of homoclinic snaking, inside this region there are two branches of localised states. The states are all invariant under the reversibility, and at each fold the number of pulses varies, so that each second successive horizontal-like branch has two additional large pulses. We remark that, in contrast to the Swift–Hohenberg equation for example, there is no variational structure in the system (8), which therefore implies there are no asymmetric stationary localised states (so-called "ladders" in a "snakes and ladders" bifurcation diagram).

In addition, we have computed stability of the states shown in Fig. 3(b) using a standard three-point uniform finite differences method and an eigenvalue solver. We have numerically found that stable branches occur similarly to results previously found for the Swift–Hohenberg system (e.g. [12, 19]) as is shown (solid lines) in Fig. 3(b). There stable branches lose stability in a fold bifurcation (filled circles) where branches of solutions with odd and even numbers of spikes annihilate each other. Examples of stable solutions are shown in Fig. 3(c); note that number of spikes correspond to ladder step.

IV. 2D SIMULATION RESULTS

To illustrate that a similar localised pattern formation mechanism is likely to apply in higher spatial dimensions we have performed simulations of the same system (8), on a large square domain with $L_{x,y} = 300$. Specifically we have used a finite difference method implemented in `matlab`, with spatial resolution 300×300. The computations were run a long time until steady state reached. The results are presented in Fig. 4.

We have found a collection of different localised patterns under the conditions of equal source and loss terms $b = r$. Samples of these can be seen in Fig. 4(a)-(c). Taking similar initial conditions that was a 10^{-2} perturbation from the homogeneous equilibrium (9) resulted in the two-spot pattern depicted in Fig. 4(a). Taking this solution as an initial conditions, a slight increase in b and r resulted in the localised 4-spot pattern depicted in Fig. 4(b). The dynamics of this process was such that each spot arises through a form of spot-splitting dynamics [31]. In a similar fashion, we slightly decreased D_1 instead. In so doing, a localised 8-spot pattern is obtained from the 4-spot pattern, see Fig. 4(c).

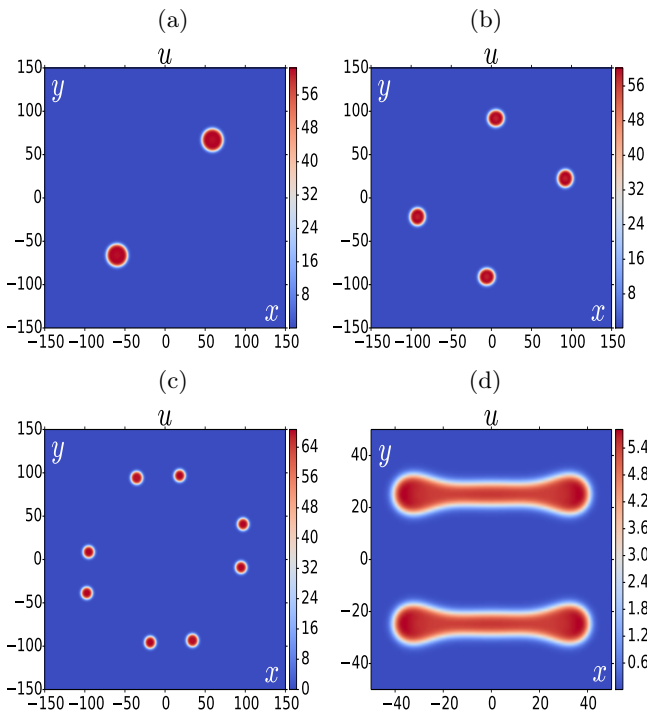In addition, we also noted that upon performing a sim-

FIG. 4. (Color online) Stable patterns for a two-dimensional square domain $L_{x,y} = 300$ on a cool-warm scale (side bar). Localised (a) 2-spot for $r = b = 10^{-4}$, $k_2 = 4 \times 10^{-3}$ and $D_1 = 0.13$, (b) 4-spot for $r = b = 5 \times 10^{-4}$, (c) 8-spot for $D_1 = 0.11$, and other parameter values as in (a). (d) 2-stripe: $r = b = 10^{-4}$, $k_2 = 0.6$, $D_1 = 0.1$, and $L_{x,y} = 100$. Other parameter values: $c = 0.1$, $h = 10^{-2}$ and $D_2 = 10$.

ilar computation but changing $b = r$ or D_1 in the other directions results in a either a completely different form of spatially extended pattern or no pattern at all. This suggests that hysteretic behaviour is taking place, which should be a consequence of an overlapping structure of stable branches similar to Fig. 3(b).

These patterns, however, are just a few examples of the spot-like patterns that we were able to find and indicate that the mechanism we have identified is likely to be robust in higher dimensions. A full exploration in the spirit of [13–15] though is left for future work. It is interesting to note though that we were unable to find any localised patterns for $b \neq r$. This suggests that well-balanced source and loss plays an important role in the (non-variational) pattern formation mechanism under investigation in higher dimensions.

On the other hand, in Fig. 4(d), a stripe-like pattern is depicted. We initially obtained a two-spot pattern as before in a smaller domain, and it was taken as an initial condition for a second run. In so doing, note that upon significantly increasing k_2 and slightly decreasing D_1 parameter values the two-spot pattern dramatically changes. Moreover, upon taking this solution as an initial

condition once again but in a much larger domain, a pattern consisting of spots and stripes emerges (not shown). Patterns as such have been observed in non-homogeneous domains, see [32, 33]. A further analysis is nevertheless also left for future work.

V. CONCLUSIONS

In summary, we have shown that canonical reaction-diffusion systems can generate localised patterns spontaneously, which, close to a relevant codimension-two point, can occur at small amplitude. In particular, taking realistic source and loss terms into account can provide conditions for a subcritical Turing bifurcation to occur. Taking the paradigm of spatial dynamics, on a long domain, the Turing bifurcation corresponds to where two complex eigenvalues collide on the imaginary axis (a Hamiltonian–Hopf bifurcation). In the presence of spatial reversibility, this provides exactly the right ingredients for the spontaneous formation of localised patterns through the so-called homoclinic snaking mechanism. Note that any realistic physical, chemical or biological systems, especially those found in nature, are likely to feature such source and loss terms.

Moreover, as argued more carefully in [34] this method of pattern formation is likely to be more robust than via the more traditional supercritical Turing instability, and hence to be chosen by nature. In the supercritical case, the pattern is always spatially extended, is born from zero amplitude and, in long domains is typically subject to further instabilities through mode interactions. In contrast for the subcritical Turing bifurcations investigated here, we find jumps to well-formed, finite amplitude patterns that are localised in the spatial domain. Due to the hysteretic nature of fold bifurcations seen in the snaking bifurcation branch, small fluctuations in parameter values or small stochastic perturbations of the kinetics would not typically destroy the localised pattern. In addition, the presence of a weak spatial inhomogeneity will result in bifurcation diagram similar to that in Fig. 3(b), but slanted so that the folds of the snake occur at different values—results not shown. For example [34] considers the system (8), in a different parameter regime, in a long (but finite) domain in 1D with a spatial gradient multiplying the bifurcation parameter k_2. The result is reminiscent of a finite portion of a slanted snake bifurcation diagram where the patterns with a higher number of spots occur for higher k_2-values. This can be explained using the concept of *slanted snaking* established by Dawes [35], where in this case the spatial gradient is replaced by a scalar field that is neutrally stable. We therefore believe the mechanism we have uncovered will prove important in explaining and predicting observations of localised patterns in certain a wide variety of physical systems, see for example [3], and will only be accentuated by spatial homogeneity.

[1] S. Kondo and T. Miura. *Science*, 329: 616–1620, 2010.

[2] J.D. Murray. *Mathematical Biology II: spatial models and biomedical applications.* Springer–Verlag, New York, 3rd. ed., 2002.

[3] V.K. Vanag and I.R. Epstein. *Chaos*, 17: 037110, 2007.

[4] A.M. Turing. *Phil. Trans. Roy. Soc. Lond. B*, 641: 37–72, 1952.

[5] H.G. Purwins, H.U. Boedeker, and Sh. Amiranashvili. *Advances in Physics*, 59(5): 485–701, 2010.

[6] J.S. Bois, F. Julicher and S.W. Grill *Phys. Rev. Lett.* 106(2): 028103, 2011.

[7] E. Khain and L.M. Sander. *Phys. Rev. Lett.*, 96(18): 188103, 2006.

[8] R. Hoyle. *Pattern Formation: An Introduction.* Cambridge University Press, Cambridge, 2006.

[9] M. Beck, J. Knobloch, D.J.B. Lloyd, B. Sandstede, T. Wagenknecht, *SIAM J. Math. Anal.* 41(3): 936–972, 2009.

[10] P.D. Woods and A.R. Champneys *Physica D* 129(3–4): 147–170, 1999.

[11] J. Burke and E. Knobloch, *Phys. Rev. E* 73(5): 056211, 2006.

[12] J. Burke and E. Knobloch. *Chaos*, 17: 037102, 2007.

[13] D. Avitabile, D.J.B. Lloyd, J. Burke, E. Knobloch, and B. Sandstede, *SIAM J. Appl. Dyn. Syst.* 9(3): 704–733, 2010.

[14] D.J.B. Lloyd, B. Sandstede, D. Avitabile and A.R. Champneys, *SIAM J. Appl. Dyn. Syst.*, 7(3): 1049–1100, 2008.

[15] D.J.B. Lloyd and B. Sandstede, *Nonlinearity* 22: 485–524, 2009.

[16] T.M. Schneider J.F. Gibson and J. Burke *Phys. Rev. Lett.*, 104(10): 104501, 2010.

[17] C. Beaume, A. Bergeon, and E. Knobloch. *Phys. Fluids*, 23(9): 094102, 2011.

[18] D. Gomila, P. Colet, M.S. Miguel, A.J. Scroggie, and G.–L. Oppo. *IEEE J.Q.E.*, 39(2): 238–244, 2003.

[19] S.M. Houghton and E. Knobloch *Phys. Rev. E* 84(1): 016204, 2011.

[20] Y. Mori, A. Jilkine and L. Edelstein–Keshet *SIAM J. Appl. Math.*, 71(4): 1402–1427, 2011.

[21] A. Yochelis, Y. Tintut, L.L. Demer adn A. Garfinkel, *New J. Phys.* 10: 055002, 2008.

[22] A. Yochelis and A. Garfinkel, *Phys. Rev. E* 77: 035204(R), 2008.

[23] D.J.B. Lloyd and H. O'Farrell, Physica D 253: 23–39, 2013.

[24] G. Iooss, and M.–C. Perouème. *J. Diff. Eqns.*, 102(1): 62–88, 1993.

[25] J. Burke and E. Knobloch. *Discrete and Continuous Dyn. Syst.*, Supplement 170–180, 2007.

[26] A.D. Dean, P.C. Matthews, S.M. Cox, and J.R. King. *Nonlinearity*, 24(12): 3323–3351, 2011.

[27] G. Kozyreff, and S.J. Chapman. *Phys. Rev. Lett.*, 97(4): 044502, 2006.

[28] R.J.H. Payne and C.S. Grierson. *PLoS ONE*, 4(12): e8337. doi:10.1371/journal.pone.0008337, 2009.

[29] M. Golubitsky and D. Schaeffer. *Singularities and Groups in Bifurcation Theory*, volume 1. New York: Springer–Verlag, 1985.

[30] V.F. Breña–Medina. PhD Thesis, University of Bristol, 2013.

[31] Y. Nishiura and D. Ueyama *Physica D* 130(1–2): 73–104, 1999.

[32] V. Breña–Medina, D. Avitabile, A.R. Champneys, and M.J. Ward, arXiv:1403.5318 [nlin.PS].

[33] R. Plaza, F. Sánchez–Garduño, P. Padilla, R.A. Barrio and P.K. Maini. *J. Dyn. Diff. Equat.*, 16(4).

[34] V. Breña–Medina, A.R. Champneys, C. Grierson, M.J. Ward, *SIAM J. Appl. Dyn. Syst.* 13(1): 210–248, 2014.

[35] J.H.P. Dawes. *SIAM J. Appl. Dyn. Syst.* 7(1): 186–206, 2008.